

Stimulated Raman adiabatic passage from an atomic to a molecular Bose-Einstein condensate

P. D. Drummond and K. V. Kheruntsyan

*Department of Physics, The University of Queensland, Brisbane,
Queensland 4072, Australia*

D. J. Heinzen

*Department of Physics, University of Texas, Austin, Texas, 78712
(March 8, 2019)*

The process of stimulated Raman adiabatic passage (STIRAP) provides a possible route for the generation of a coherent molecular Bose-Einstein condensate (BEC) from an atomic BEC. We analyze this process in a full three-dimensional, multi-mode theory, including atom-atom interactions and non-resonant intermediate levels. We find that the process is feasible, but at larger Rabi frequencies than anticipated from a crude single-mode lossless analysis, due to two-photon dephasing caused by the atomic interactions. We then identify optimal strategies in STIRAP allowing one to maintain high conversion efficiencies with smaller Rabi frequencies and under experimentally less demanding conditions.

PACS numbers: 03.75.Fi, 05.30.Jp, 03.65.Ge.

I. INTRODUCTION

Coherent conversion of an atomic to a molecular Bose-Einstein condensate (BEC) is a first step towards ‘superchemistry’ [1], which is the stimulated emission of molecules in a chemical reaction. A number of studies of this [2–4] have shown that direct conversion via Raman photoassociation [5] appears feasible, based on stimulated free-bound and bound-bound transitions in the presence of two laser fields of different frequencies [6]. Here pairs of atoms from the two-atom continuum of the ground electronic potential are transferred – via an excited bound molecular state – to a bound molecular state of a lower energy in the ground potential. Raman photoassociation allows coupling to a single molecular state, which can be selected by the Raman laser frequencies. Practical estimates using available lasers and transitions indicate that coherent transfer may be limited by spontaneous emission from the intermediate molecular excited electronic state. Another mechanism that can result in coupled atomic-molecular BEC systems [7] is based on Feshbach resonances [8]. However, realistic analysis and experimental implementations [9] indicate that the loss processes due to inelastic atom-molecule collisions occur at a significant rate.

A possible route towards minimizing losses and decoherence from spontaneous emission in photoassociation is stimulated Raman adiabatic passage (STIRAP) [10], in which a counter-intuitive pulse sequence is used, where

the first input pulse couples the molecular levels – even when there are no molecules present. In this situation, a dark superposition state is formed, due to interference effects between the atomic and molecular electronic ground states. This minimizes the probability of a real transition to the molecular excited state, and hence reduces spontaneous emission. Previous analyses of this problem have not taken into account losses, collisions, or the full three-dimensional structure of the two Bose condensates in a trap.

In this paper, we provide an analysis which is relevant in a physically appropriate model that does include the known physics of spontaneous emission losses, *s*-wave scattering processes and spatial diffusion of the condensates. The result is that the STIRAP process appears feasible at high laser pulse intensities, provided the Rabi frequency is much greater than the two-photon detuning due to mean-field interactions. We give a detailed numerical calculation based on a modified mean-field (Gross-Pitaevskii type) theory, including couplings to non-resonant intermediate levels, and show how the results scale with the two-photon detuning, pulse duration and Raman pulse intensities. An optimal situation is found by considering an off-resonance operation and different effective Rabi frequencies in the two Raman channels. We show that these strategies can greatly enhance the conversion efficiency for given laser intensities, thus making the experimental requirements much more feasible.

II. COUPLED GROSS-PITAEVSKII EQUATIONS FOR STIRAP

We start by considering the theory of coherently interacting atomic and molecular condensates needed to describe this process [1,3], and assume a specific coupling mechanism based on stimulated free-bound Raman transitions [6], in which two atoms of energy E_1 collide to form a molecule of energy E_2 , with an excited molecular state forming as an intermediate step. The Raman coupling is induced by two laser fields of frequencies ω_1 and ω_2 , and becomes resonant when the Raman detuning $\delta = (2E_1 - E_2)/\hbar - (\omega_2 - \omega_1)$ goes to zero. This allows coupling to a single molecular state, which can be

selected by the Raman laser frequencies.

We derive the atom-molecule coupling for a simplified model of the two-body interaction [1,11], in which the atoms interact in their electronic ground state through a single Born-Oppenheimer potential $V_g(R)$. Molecules are formed in a single bound vibrational state of energy E_2 with radial wave function $u_2(R)$. Two free atoms with zero relative kinetic energy have a total energy $2E_1$, and a relative radial wave function $u_1(R)$, normalized so that asymptotically $u_1 \propto (1 - a_1/R)$. We assume that the laser field has two frequency components, with $\mathbf{E} = \text{Re} \sum [\mathbf{E}^{(i)} \exp(i\omega_i t)]$, $i = 1, 2$. Each couples the ground electronic state to a single electronically excited state described by a potential $V_e(R)$, with ‘bare’ electronic Rabi frequencies $\Omega_i^{(el)}(\mathbf{R}) = \mathbf{d}_{3i}(\mathbf{R}) \cdot \mathbf{E}^{(i)}/\hbar$, where $\mathbf{d}_{3i}(\mathbf{R})$ is the molecular electric dipole matrix element with a nuclear separation of \mathbf{R} . The excited state has vibrational levels $|v'\rangle$ with energies $E_{v'}$ and radial wave functions $u_{v'}(R)$. All bound levels are normalized so that $\int d^3\mathbf{R}|u_{v'}|^2 = \int d^3\mathbf{R}|u_2|^2 = 1$.

We consider the case of near resonant transitions $1 \rightarrow v' \rightarrow 2$ and denote the resonant excited vibrational level v' via index 3 (see Fig. 1). The usual quantum field theory Hamiltonian [12] for noninteracting atomic ($i = 1$) and molecular ($i = 2, 3$) species, in well-defined internal states described by annihilation operators $\hat{\Psi}_i$, is given by:

$$\hat{H}^{(0)} = \int d^3\mathbf{x} \sum_{i=1}^3 \left[\frac{\hbar^2}{2m_i} |\nabla \hat{\Psi}_i(\mathbf{x})|^2 + V_i(\mathbf{x}) \hat{\Psi}_i^\dagger(\mathbf{x}) \hat{\Psi}_i(\mathbf{x}) \right]. \quad (1)$$

Here m_i ($i = 1, 2, 3$) are the masses, $m_{2,3} = 2m_1$, and $V_i(\mathbf{x})$ is the trapping potential including the internal energy for the i -th species, where we define $V_i(0) = E_i$.

Including s -wave scattering processes and laser induced particle inter-conversion, together with the assumption of a momentum cut-off, results in the following terms in the effective interaction Hamiltonian:

$$\hat{H}_{int}^{(s)} = \frac{\hbar}{2} \int d^3\mathbf{x} \sum_{ij} U_{ij} \hat{\Psi}_i^\dagger(\mathbf{x}) \hat{\Psi}_j^\dagger(\mathbf{x}) \hat{\Psi}_j(\mathbf{x}) \hat{\Psi}_i(\mathbf{x}), \quad (2)$$

$$\hat{H}_{int}^{(1-3)} = \int d^3\mathbf{x} \left[\frac{-\hbar\Omega_1}{2\sqrt{2}} e^{-i\omega_1 t} \hat{\Psi}_1^\dagger(\mathbf{x}) \hat{\Psi}_3^\dagger(\mathbf{x}) + H.c. \right], \quad (3)$$

$$\hat{H}_{int}^{(2-3)} = \int d^3\mathbf{x} \left[\frac{-\hbar\Omega_2}{2} e^{-i\omega_2 t} \hat{\Psi}_2^\dagger(\mathbf{x}) \hat{\Psi}_3^\dagger(\mathbf{x}) + H.c. \right]. \quad (4)$$

Here $\Omega_i = \int d^3\mathbf{R} \Omega_i^{(el)}(\mathbf{R}) u_3^*(R) u_i(R) \approx \overline{\Omega}_i^{(el)} I_{i,3}$ ($i = 1, 2$) are the molecular Rabi frequencies. These can be treated using the Franck-Condon overlap integrals $I_{i,3} = \int d^3\mathbf{R} u_3^*(R) u_i(R)$, if we take $\overline{\Omega}_i^{(el)}$ as the mean electronic Rabi frequency. We note that Ω_1 , which connects the atomic and molecular condensates, has units of $s^{-1}m^{-3/2}$, and must be multiplied by the atomic condensate amplitude to obtain a true Rabi frequency. The couplings U_{ij} in the diagonal case are given by

$U_{ii} = 4\pi\hbar a_i/m_i$, where a_i is the i -th species s -wave scattering length, while the non-diagonal terms are given by $U_{ij} = U_{ji} = 2\pi\hbar a_{ij}/\mu_{ij}$, where a_{ij} is the inter-species scattering length and $\mu = m_i m_j / (m_i + m_j)$ is the reduced mass.

In addition, we account for losses from each state, at a rate γ_i . The resulting Heisenberg equations for the field operators are treated within the mean-field approximation, in which the operators are replaced by their mean values, and a factorization is assumed. This approximation is expected to be valid at sufficiently high density. Corrections due to quantum correlations [13] have been treated in greater detail elsewhere [14]. Next, we introduce rotating frame detunings, defined so that:

$$\begin{aligned} 2\Delta_1(\mathbf{x}) &= (E_3 - 2V_1(\mathbf{x}))/\hbar - \omega_1, \\ \Delta_2(\mathbf{x}) &= (E_3 - V_2(\mathbf{x}))/\hbar - \omega_2, \\ \Delta_3(\mathbf{x}) &= E_3 - V_3(\mathbf{x}). \end{aligned} \quad (5)$$

In the case of uniform condensates, $V_i(\mathbf{x})$ are equal to $V_i(\mathbf{x}) = E_i$, and $\Delta_3 = 0$.

This results in the following set of Gross-Pitaevskii type of equations for the mean-field amplitudes, in rotating frames such that $\psi_i = \langle \hat{\Psi}_i \rangle \exp[i(E_i + \Delta_i(0))t/\hbar]$:

$$\begin{aligned} \frac{\partial \psi_1(\mathbf{x}, t)}{\partial t} &= i\Delta_1^{GP} \psi_1 + \frac{i\Omega_1}{\sqrt{2}} \psi_3 \psi_1^*, \\ \frac{\partial \psi_2(\mathbf{x}, t)}{\partial t} &= i\Delta_2^{GP} \psi_2 + \frac{i\Omega_2}{2} \psi_3, \\ \frac{\partial \psi_3(\mathbf{x}, t)}{\partial t} &= i\Delta_3^{GP} \psi_3 + \frac{i\Omega_1^*}{2\sqrt{2}} \psi_1^2 + \frac{i\Omega_2^*}{2} \psi_2, \end{aligned} \quad (6)$$

Here Δ_j^{GP} is the j -th Gross-Pitaevskii mean-field detuning in the rotating frame, defined so that:

$$\Delta_j^{GP}(\mathbf{x}, t) = \Delta_j(\mathbf{x}) + \frac{\hbar}{2m_j} \nabla^2 - \sum_{k=1}^3 U_{jk} |\psi_k|^2 + i \frac{\gamma_j}{2}. \quad (7)$$

We also introduce the two-photon laser detuning at trap center:

$$\delta \equiv \Delta_2(0) - 2\Delta_1(0) = -(E_2 - 2E_1)/\hbar + (\omega_1 - \omega_2). \quad (8)$$

In addition to losses due to spontaneous emission from the electronic excited states, rotationally or vibrationally inelastic atom-molecule collisions may also give rise to losses. The magnitude of these rates is presently unknown, and we neglect them here. We note that these rates should decrease rapidly with increasing molecular binding energy and go to zero in the molecular ground state, so that it should be possible to obtain a very low rate by selecting the coupling to a deeply bound molecular level. This approximation means that we will set $\gamma_i = \gamma \delta_{3i}$ in the following treatment, where δ_{ij} is the Kronecker delta-function.

The simplest STIRAP scheme employs exact tuning of the laser frequencies to the bare state resonances, i.e., $\Delta_1(0) = \Delta_2(0) = 0$. This, however, is not necessarily required as the STIRAP can still occur with detuned intermediate levels. Moreover, as we show below, in BEC environments, the off-resonance operation turns out to be more efficient if the detunings compensate for the phase shifts due to mean-field energies. In effect this is equivalent to a renormalized two-photon “on-resonant” operation in which $\Delta_2^{GP}(\mathbf{x}, 0) - 2\Delta_1^{GP}(\mathbf{x}, 0) \approx 0$.

If, instead of considering near-resonance coupling, we consider a large intermediate level detuning so that the excited state can be adiabatically eliminated, we recover the basic terms in the set of equations analyzed in [1]. Simultaneously, this would give us the previously known result [11] for the laser induced modification to the scattering length a_1 occurring in a simple single-laser photoassociation of pairs of atoms, thus justifying the above form of the interaction Hamiltonian. In the present paper, however, we assume that the detunings Δ_i are small compared to the characteristic separation between the vibrational levels so that all other vibrational levels can be neglected. The near-resonant excited level is treated explicitly, rather than eliminated adiabatically as in [1].

III. STIRAP IN A BEC

Before carrying out simulations of the full 3D equations in a trap, it is instructive to start with a simplified version of the theory - in which there are no kinetic energy terms. We expect this approximation to be valid in the Thomas-Fermi limit of large, relatively dense condensates, which is a regime of much current experimental interest. This is described by the following set of equations:

$$\begin{aligned} \frac{\partial\psi_1(\mathbf{x}, t)}{\partial t} &= i\Delta_1^{TF}\psi_1 + \frac{i\Omega_1}{\sqrt{2}}\psi_3\psi_1^*, \\ \frac{\partial\psi_2(\mathbf{x}, t)}{\partial t} &= i\Delta_2^{TF}\psi_2 + \frac{i\Omega_2}{2}\psi_3, \\ \frac{\partial\psi_3(\mathbf{x}, t)}{\partial t} &= i\Delta_3^{TF}\psi_3 + \frac{i\Omega_1^*}{2\sqrt{2}}\psi_1^2 + \frac{i\Omega_2^*}{2}\psi_2, \end{aligned} \quad (9)$$

where we have introduced as an effective Thomas-Fermi limit frequency shift,

$$\Delta_j^{TF}(\mathbf{x}, t) = \Delta_j(\mathbf{x}) - \sum_{k=1}^3 U_{jk}|\psi_k|^2 + i\frac{\gamma_j}{2}. \quad (10)$$

This corresponds to the treatment given in [10], except that we explicitly include the loss term γ due to spontaneous emission, the s -wave scattering processes due to U_{ij} , and the Franck-Condon integrals into the coupling coefficients for the free-bound and bound-bound transitions.

In order to understand how this is related to the usual STIRAP technique in a three-level Λ atomic system, we

introduce a new wave-function $\psi_m = \psi_1/\sqrt{2}$, which corresponds to the coherent amplitude of a (virtual) molecular condensate with the same number of atoms as in the atomic BEC. We then introduce a Bose-stimulated Rabi frequency, which includes a local coherent BEC amplitude for the first free-bound transition: $\tilde{\Omega}_1 = \psi_1^*\Omega_1$. This leads to the equations:

$$\begin{aligned} \frac{\partial\psi_m(\mathbf{x}, t)}{\partial t} &= i\Delta_1^{TF}\psi_m + \frac{i\tilde{\Omega}_1}{2}\psi_3, \\ \frac{\partial\psi_2(\mathbf{x}, t)}{\partial t} &= i\Delta_2^{TF}\psi_2 + \frac{i\Omega_2}{2}\psi_3, \\ \frac{\partial\psi_3(\mathbf{x}, t)}{\partial t} &= i\Delta_3^{TF}\psi_3 + \frac{i\tilde{\Omega}_1^*}{2}\psi_m + \frac{i\Omega_2^*}{2}\psi_2. \end{aligned} \quad (11)$$

These are precisely the usual STIRAP equations, except with additional detunings coming from the mean-field interactions, and a Rabi frequency in the first transition which is proportional to the amplitude of the atomic BEC wave-function. In practise, the Rabi frequency may have an additional space-dependence due to the spatial variation of the laser phase and intensity. We therefore conclude that, provided we can satisfy the normal adiabatic STIRAP requirements of slow time-variation in the *effective* Rabi frequencies in the above equations, the technique will also work for a BEC. This is a simpler proof than previously [10]. In particular, we can immediately deduce the expected solution for real Rabi frequencies in the adiabatic limit:

$$\begin{aligned} \psi_1(\mathbf{x}, t) &= \psi_1(\mathbf{x}, 0)\cos(\theta), \\ \psi_2(\mathbf{x}, t) &= \psi_1(\mathbf{x}, 0)\sin(\theta)/\sqrt{2}, \\ \psi_3(\mathbf{x}, t) &= 0. \end{aligned} \quad (12)$$

Here the space dependent mixing angle $\theta(\mathbf{x}, t)$ is obtained from the ratio of effective Rabi frequencies:

$$\tan(\theta) = \frac{\tilde{\Omega}_1}{\Omega_2} = \frac{\psi_1\Omega_1}{\Omega_2} = \left[\sqrt{\frac{\psi_1^2(\mathbf{x}, 0)\Omega_1^2}{\Omega_2^2} + \frac{1}{4}} - \frac{1}{2} \right]^{1/2}. \quad (13)$$

We can see that *initially*, while ψ_1 is still close to its initial value, the mixing angle is close to its expected value in normal STIRAP, since $\tan(\theta) \approx \psi_1(\mathbf{x}, 0)\Omega_1/\Omega_2$. However, at the final stages of the adiabatic passage, the nonlinear effects due to the atom-molecular coupling become important. As the atomic BEC amplitude only varies on the time-scale of the input fields, the nonlinear atom-molecular coupling term by itself should not introduce new adiabatic restrictions. However, there will be time-dependent detunings introduced by the mean-field terms.

Finally, we can see that similar conclusions can also be reached in a non-uniform BEC, by replacing the uniform detunings with appropriate Gross-Pitaevskii detunings, that include the spatial potentials. In a typical BEC cooled in the Thomas-Fermi regime, we expect the kinetic energy terms to have relatively small effects.

STIRAP can therefore be implemented as usually by using two laser pulses applied in counterintuitive order. We choose Gaussian pulses of the form

$$\bar{\Omega}_i^{(el)}(t) = \Omega_i^{(el,0)} \exp[-(t - t_i)^2/T^2], \quad (i = 1, 2), \quad (14)$$

or

$$\Omega_i(t) = \Omega_i^{(0)} \exp[-(t - t_i)^2/T^2], \quad (15)$$

where the peak values are related as follows: $\Omega_i^{(0)} = \Omega_i^{(el,0)} I_{i,3}$. The pulse at frequency ω_2 is applied first, with the center at t_2 , while the second pulse at frequency ω_1 is delayed by αT , i. e.,

$$t_1 - t_2 = \alpha T, \quad (16)$$

where α is the delay coefficient, and T is the pulse duration, which we assume is the same for both pulses.

In terms of the Rabi frequencies, the adiabatic condition for STIRAP now reads as [15]:

$$\Omega(t)\Delta\tau \gg \sqrt{1 + |2\Delta_1^{TF} - \Delta_3^{TF}|}\Delta\tau, \quad (17)$$

where $\Omega(t) = \sqrt{|\tilde{\Omega}_1(t)|^2 + |\Omega_2(t)|^2}$ is the rms Rabi frequency, $\Delta\tau$ is the duration during which the pulses overlap, and $(2\Delta_1^{TF} - \Delta_3^{TF})$ simply corresponds to the detuning of the single-photon transition. However, there is a second condition, which is often not stated explicitly. This is that STIRAP requires an effective two-photon resonance, to avoid dephasing between the initial and final states in the dark-state superposition. The two-photon resonance condition is different from the usual STIRAP case, since a detuning of Δ_1^{TF} causes a phase rotation *both* in ψ_m and in $\tilde{\Omega}_1$ as well, since this also includes a phase term from the condensate. As a result, the necessary condition for two-photon resonance is therefore:

$$|\Delta_2^{TF} - 2\Delta_1^{TF}|\Delta\tau \ll 1. \quad (18)$$

This leads to a third condition, which shows that there is a lower bound to the allowed Rabi frequency in order to have STIRAP occurring in the presence of mean-field dephasing effects:

$$\Omega(t) \gg |\Delta_2^{TF} - 2\Delta_1^{TF}|. \quad (19)$$

As is usually the case in STIRAP, these conditions cannot be satisfied very early or late in the pulse sequence, when the Rabi frequencies are small; but they should be satisfied over most of the STIRAP interaction, and over most of the condensate volume. For simplicity, we will apply these conditions to the peak Rabi frequency $\Omega^{(0)}$, and to the total pulse duration T . Further, since $\tilde{\Omega}_1$ is itself a function of the STIRAP evolution, we introduce an effective first Rabi frequency, defined in terms of the initial density $n_1(0) = |\psi_1(0)|^2$. This is

γ	$7.4 \times 10^7 \text{ s}^{-1}$
$n_1(0)$	$4.3 \times 10^{20} \text{ m}^{-3}$
$\Omega_1^{(eff,0)} = \Omega_2^{(eff,0)}$	$2.1 \times 10^7 \text{ s}^{-1}$
T	10^{-4} s

TABLE I. Typical parameter values for efficient STIRAP.

an upper bound to the stimulated Rabi frequency; thus $\Omega_1^{(eff)}(t) = \sqrt{n_1(0)}\Omega_1(t) \geq \tilde{\Omega}_1(t)$ (and sometimes we write $\Omega_2^{(eff)}(t) = \Omega_2(t)$, for uniformity), where

$$\Omega_i^{(eff)}(t) = \Omega_i^{(eff,0)} \exp[-(t - t_i)^2/T^2], \quad (i = 1, 2), \quad (20)$$

where $\Omega_1^{(eff,0)} = \Omega_1^{(el,0)} I_{1,3} \sqrt{n_1(0)}$ and $\Omega_2^{(eff,0)} = \Omega_2^{(el,0)} I_{2,3}$.

A typical pulse sequence is shown in Fig. 2. From the definition of Ω_i , the Franck-Condon overlap integrals are an important issue from the point of view of employing a realistic set of parameters. Since the overlap integrals enter into the definition of the effective Rabi frequencies, their values will affect the adiabatic condition rewritten in terms of the “bare” electronic Rabi frequencies $\bar{\Omega}_i^{(el)}$. We will analyze this in more detail in the next section.

IV. UNIFORM CONDENSATE RESULTS

We start by considering a uniform condensate, described by a similar equation to the Thomas-Fermi case, except with a uniform trap potential for simplicity:

$$\begin{aligned} \frac{\partial\psi_m(\mathbf{x}, t)}{\partial t} &= i\Delta_1^{TF}(0)\psi_m + \frac{i\tilde{\Omega}_1}{2}\psi_3, \\ \frac{\partial\psi_2(\mathbf{x}, t)}{\partial t} &= i\Delta_2^{TF}(0)\psi_2 + \frac{i\Omega_2}{2}\psi_3, \\ \frac{\partial\psi_3(\mathbf{x}, t)}{\partial t} &= i\Delta_3^{TF}(0)\psi_3 - \frac{i\tilde{\Omega}_1^*}{2}\psi_m - \frac{i\Omega_2^*}{2}\psi_2. \end{aligned} \quad (21)$$

Here the uniform detuning term $\Delta_1^{TF}(0)$ is defined as the Thomas-Fermi detuning, evaluated at the trap center. We start by considering a uniform condensate in which the *s*-wave scattering interactions are negligible (i.e., $U_{ij} = 0$), and assume exact resonances with respect to bare state transitions, $\Delta_1 = \Delta_2 = 0$. We first simulate the above simplified equations (21) with an initial condition of a pure atomic condensate. This model is more realistic than that of M. Mackie et al. [10], as it includes spontaneous emission. We find that including the loss term γ imposes restrictions on the effective Rabi frequencies $\Omega_i^{(eff,0)}$ and the duration of the pulses T .

The results are best understood with reference to Table I, which gives the values of typical STIRAP parameters characteristic of a condensate of ^{87}Rb atoms [1,5]), and corresponding to the pulse sequence in Fig. 2.

Taking the values of the parameters in Table I, and an optimum delay coefficient of $\alpha \simeq 1.5$, gives $\eta \simeq 0.96$ or about 96% efficiency of conversion of atomic BEC into molecular BEC, even including the upper level spontaneous emission. Here, the conversion efficiency η is defined as the fraction of the initial number of atoms $n_1(0)$ converted into molecules

$$\eta = \frac{2n_2(\infty)}{n_1(0)}, \quad (22)$$

where $n_2(\infty)$ is the final number of molecules. This accounts for the fact that n_1 atoms can produce $n_1/2$ molecules at best.

For comparison, using smaller Rabi frequencies, $\Omega_i^{(eff,0)} = 2.1 \times 10^6 \text{ s}^{-1}$, and a larger value of $T = 10^{-3} \text{ s}$, so that the product $\Omega_i^{(eff,0)}T$ still has the previous value $\Omega_i^{(eff,0)}T = 2.1 \times 10^3$, gives a maximum conversion efficiency of $\eta \simeq 0.83$, with a new optimum delay coefficient $\alpha \simeq 1.2$. This is smaller than in the previous example. In order to reach the same efficiency as before, one has to further increase the pulse durations (up to $T = 10^{-2} \text{ s}$), i.e. enter into a deeper adiabatic regime. In the absence of the spontaneous emission term, the conversion efficiencies would not be different in these two examples.

In other words, in this simplified model it is possible to have effective Rabi frequencies smaller than the spontaneous emission rate γ , provided the duration of the pulses is long enough. As usual, we can understand this physically as implying that the upper level is never actually occupied for very slowly varying adiabatic pulses. Hence, just as in the case of atomic STIRAP, we can ignore spontaneous emission from the upper level provided that we use very slowly varying pulses which are sufficiently deep in the adiabatic limit. As we see in the following calculations, the problem with this strategy is that very long pulses will tend to cause violations of the two-photon resonance condition, in the presence of mean-field interactions.

A. Effects of the mean-field energies

We now wish to include the mean-field energy terms, and first restrict our analysis to the atom-atom scattering processes. We consider a characteristic value of $U_{11} = 4.96 \times 10^{-17} \text{ m}^3/\text{s}$ corresponding to the scattering length of ^{87}Rb atoms [16] $a_1 = 5.4 \text{ nm}$ ($m_1 = 1.443 \times 10^{-25} \text{ kg}$). Together with the choice of the initial atomic density $n_1(0)$ as before (see Table I), the value of U_{11} sets up a characteristic dephasing time scale

$$t_{ph} = [U_{11}n_1(0)]^{-1}, \quad (23)$$

equal in this case to $t_{ph} \simeq 4.7 \times 10^{-5} \text{ s}$. The pulse duration T must be smaller than or of the order of the dephasing time, in order to permit STIRAP, otherwise the two-photon resonance condition will not be satisfied.

U_{11}	$4.96 \times 10^{-17} \text{ m}^3/\text{s}$
U_{12}	$-6.44 \times 10^{-17} \text{ m}^3/\text{s}$
U_{22}	$2.48 \times 10^{-17} \text{ m}^3/\text{s}$
U_{3i}	0

TABLE II. Typical mean-field interaction potentials in Rubidium condensates.

Thus, including atom-atom scattering imposes an upper limit to the pulse duration, so that T has now to satisfy $T \lesssim t_{ph} \simeq 10^{-5} - 10^{-4} \text{ s}$. But this restriction means that one can no longer use *longer* pulse durations for *small* values of $\Omega_i^{(eff,0)}$, while still maintaining high conversion efficiency. As a result, the adiabatic condition $\Omega_i^{(eff,0)}T \gg 1$, with the restriction of $T \lesssim 10^{-5} - 10^{-4} \text{ s}$, requires high peak values of the effective Rabi frequencies: $\Omega_i^{(eff,0)} \gtrsim 10^7 \text{ s}^{-1}$.

In order to satisfy this combination of requirements, we use typical parameter values given in Table I, with $U_{11} = 4.96 \times 10^{-17} \text{ m}^3/\text{s}$. Simulating Eqs. (21) with these parameter values and with all other couplings U_{ij} set to zero, gives a maximum of $\eta \simeq 0.95$ conversion efficiency, for the optimum delay coefficient of $\alpha \simeq 1.5$.

As the next step, one can include the mean-field energies due to atom-molecule (U_{12} , U_{13}) and molecule-molecule (U_{22} , U_{23} , U_{33}) scattering processes. Considering the fact that the excited molecular state never gets highly populated in STIRAP, only processes described by U_{12} and U_{22} are to be taken into account here. Provided that the scattering lengths for these processes are of the same order of magnitude as the atom-atom scattering length, these terms do not lead to a dramatic change in the conversion efficiency.

To account for the most recent experimental data on ultracold atom-molecule scattering in a ^{87}Rb condensate [5], we have included the U_{12} term with $a_{12} = -9.346 \text{ nm}$. In addition, we include the U_{22} term with an assumption that $a_2 = a_1$ and set $U_{3i} = 0$ since these are currently not known. The resulting values of U_{ij} are summarized in Table II. The results of simulations are given in Fig. 3, where we see about 93% ($\eta \simeq 0.93$) conversion of the atomic condensate into the condensate of molecules, for $\Omega_1^{(eff,0)} = \Omega_2^{(eff,0)} = 2.1 \times 10^7 \text{ s}^{-1}$, $T = 10^{-4} \text{ s}$, and $\alpha \simeq 1.5$. This figure also includes the analytic theory calculated in the adiabatic limit for comparison, and shows that for these parameters, the results of the numerical simulation are close to those from the adiabatic theory.

Thus, we conclude that even including the mean field energies STIRAP can be carried out, provided one uses faster time scales than in the absence of the *s*-wave scattering. As a consequence the effective Rabi frequencies have to be kept at a rather high value. Characteristic results for comparison are summarized in Fig. 4, where we plot conversion efficiency η versus the relative delay coefficient α , for cases where *s*-wave scattering are present or absent, and for different values of the effective Rabi

frequencies and pulse durations T .

Figure 4 (a) shows a reasonably efficient conversion, in the absence of mean-field interactions, but including losses. As expected, spontaneous emission losses are reduced, and efficiency is improved further by the use of longer pulses, further into the adiabatic limit, as in Fig. 4 (b). However, the more realistic example given in Fig. 4 (c) which includes mean-field interactions shows rather poor conversion, especially when we use smaller effective Rabi frequencies, $\Omega_1^{(eff,0)} = \Omega_2^{(eff,0)} = 2.1 \times 10^6 \text{ s}^{-1}$, as shown by the full line where maximum $\eta \simeq 0.12$ at optimum $\alpha \simeq 0.7$. This is caused by the effective two-photon detunings induced by the mean-field interactions. The situation is made even worse rather than better in Fig 4 (d) when longer pulses are chosen, giving more time for two-photon detunings to occur.

To be more specific about values of the effective Rabi frequencies we recall that the definition of $\Omega_i^{(eff)}$ involves the Franck-Condon overlap integrals $I_{i,3}$ and “bare” electronic Rabi frequencies $\bar{\Omega}_i^{(el)} = |\bar{\mathbf{d}}_M \cdot \mathbf{E}_i|/\hbar$. Given the values of $\bar{\mathbf{d}}_M$ and $I_{i,3}$ which are specific for particular dimer species involved, the size of $\Omega_i^{(eff,0)}$ can be translated to the intensities of the Raman lasers. Considering $^{87}\text{Rb}_2$ as an example, and using a characteristic values of the corresponding Franck-Condon integrals, $|I_{1,3}| \simeq 10^{-14} \text{ m}^{3/2}$ and $|I_{2,3}| \simeq 0.1$ [1], the magnitudes of $\Omega_1^{(eff,0)} = \Omega_2^{(eff,0)} = 2.1 \times 10^7 \text{ s}^{-1}$ translate to peak values of the “bare” Rabi frequencies equal to $\Omega_1^{(el,0)} = 10^{11} \text{ s}^{-1}$ (for $n_1(0) = 4.3 \times 10^{20} \text{ m}^{-3}$) and $\Omega_2^{(el,0)} = 2.1 \times 10^8 \text{ s}^{-1}$. The peak Rabi frequency of $\Omega_1^{(el,0)} = 10^{11} \text{ s}^{-1}$ for the free-bound transition would be realized with a 1 W laser power and a waist size of about 10 μm , which is not impossible – but much higher than we would estimate without the combined effects of spontaneous emission and collisional processes. Another obvious problem here is that the waist size of 10 μm is comparable to characteristic spatial extend of current BECs in a trap.

In summary, our analysis shows that the relatively small overlap integrals for the free-bound transitions, together with the mean-field interaction detunings, can require rather high intensity of the ω_1 -laser for obtaining high conversion efficiencies.

B. Off-resonance operation

In order to allow one to operate under less demanding laser powers or *smaller* Rabi frequencies (e.g. $\Omega_1^{(eff,0)} = \Omega_2^{(eff,0)} = 2.1 \times 10^6 \text{ s}^{-1}$) – while still maintaining efficient conversion – we now consider the role of the detunings Δ_1 and Δ_2 in the off-resonance regime of operation. In effect, this approach relies on compensating for the phase shifts due to the mean field energies, and tuning the free-bound and bound-bound transitions to a “true” resonance. The physics behind this is that in BEC environments it is not

appropriate to consider transitions with respect to single-particle bare energies E_i . Rather, the relevant energies and therefore the effective resonances have to take into account the mean-field energy contributions due to self- and cross-interactions between the condensates.

More specifically, it is the *two-photon* detuning δ that has to be adjusted to the *relative* phase between the atomic and molecular condensates. Alternatively speaking, by tuning the two-photon detuning to compensate for the net mean-field energy, one reduces the effect of dephasing since the effective dephasing time becomes longer compared to the pulse durations. The problem, however, is more complicated because the mean field energy is changed dynamically as the populations of the atomic and the molecular condensate themselves are being changed during STIRAP. As a crude estimate of an appropriate value of δ one can simply choose it to compensate the *initial* mean field energy in the atomic condensate. This approach – employed for smaller Rabi frequencies than before – can substantially improve the conversion efficiency, compared to the case of zero two-photon detuning.

To show this we have carried out simulations with ten times smaller Rabi frequencies than before (i.e. with $\Omega_i^{(eff,0)} = 2.1 \times 10^6 \text{ s}^{-1}$), corresponding to a decrease of the Raman laser intensities by a factor of 100. The results are summarized in Fig. 5, where we plot the conversion efficiency η versus δ , for $T = 10^{-4} \text{ s}$ and different delay coefficients α .

As we see, by varying the two-photon detuning and tuning it to the optimum value can improve the conversion efficiency by about a factor of two or more, for a range of values of the delay coefficient. Furthermore, as the effective dephasing time is increased when the contribution of the mean field energies is compensated by δ , one can further improve the results by employing longer pulse durations. More generally, the problem of finding a set of values of T , α , and δ that maximize the conversion efficiency, for given values of the effective Rabi frequencies, is now transformed to an optimization problem.

C. Asymmetric effective Rabi frequencies

We now wish to explore an alternative strategy for improving the conversion efficiency under experimentally less demanding conditions of smaller Rabi frequencies. We consider the effects of non-equal effective Rabi frequencies.

Using the earlier given characteristic values of the Franck-Condon overlap integrals, $|I_{1,3}| \simeq 10^{-14} \text{ m}^{3/2}$ and $|I_{2,3}| \simeq 0.1$, we can estimate that the moderate magnitudes of $\Omega_1^{(eff,0)} = \Omega_2^{(eff,0)} = 2.1 \times 10^6 \text{ s}^{-1}$ translate to the following peak values of the bare Rabi frequencies: $\Omega_1^{(el,0)} = 10^{10} \text{ s}^{-1}$ (for $n_1(0) \sim 4.3 \times 10^{20} \text{ m}^{-3}$) and $\Omega_2^{(el,0)} = 2.1 \times 10^7 \text{ s}^{-1}$. As we see, while this corresponds to equal *effective* Rabi frequencies, however, the absolute

$\Omega_2^{(el,0)} \text{ (s}^{-1}\text{)}$	$T \times 10^{-4} \text{ s}$	α	$\delta \times 10^4 \text{ s}^{-1}$	η
1.5×10^7	0.987	0.753	3.58	0.257
2.1×10^7	0.966	0.795	3.57	0.331
3×10^7	1.05	0.882	3.44	0.391
5×10^7	1.29	1.05	3.11	0.437
7.5×10^7	1.49	1.19	2.92	0.453
10^8	1.61	1.30	2.83	0.459
2×10^8	1.86	1.53	2.71	0.467
10^9	2.32	1.98	2.59	0.474
10^{10}	2.58	2.51	2.93	0.486

TABLE III. Optimum STIRAP parameters for: $\Omega_1^{(el,0)} = 10^{10} \text{ s}^{-1}$, $|I_{1,3}| = 10^{-14} \text{ m}^{3/2}/\text{s}$, and $n_1(0) = 4.3 \times 10^{20} \text{ m}^{-3}$, so that $\Omega_1^{(eff,0)} = 2.1 \times 10^6 \text{ s}^{-1}$ in all cases; different values of $\Omega_2^{(eff,0)} = I_{1,3}\Omega_2^{(el,0)}$ are taken for $|I_{1,3}| = 0.1$ and $\Omega_2^{(el,0)}$ ranging from 1.5×10^7 to 10^{10} s^{-1} .

values of the corresponding *bare* Rabi frequencies are *not* equal. The limitation on laser intensities refers primarily to the free-bound transition, whose bare Rabi frequency $\Omega_1^{(el,0)}$ is higher.

As far as the second Rabi frequency $\Omega_2^{(el,0)}$ is concerned, one can in principle increase its magnitude up to the same value as $\Omega_1^{(el,0)}$, i.e. $\Omega_2^{(el,0)} = 10^{10} \text{ s}^{-1}$, thus maintaining experimentally similar and reasonably high intensities for both lasers. Under these conditions, and for the same values of the Franck-Condon overlap integrals and $n_1(0)$, we would have

$$\begin{aligned} \Omega_1^{(el,0)} &= 10^{10} \text{ s}^{-1}, \quad \Omega_1^{(eff,0)} = 2.1 \times 10^6 \text{ s}^{-1}, \\ \Omega_2^{(el,0)} &= 10^{10} \text{ s}^{-1}, \quad \Omega_2^{(eff,0)} = 10^9 \text{ s}^{-1}. \end{aligned} \quad (24)$$

We can now ask the question of what happens in STIRAP with *different* effective Rabi frequencies, and whether one can achieve higher conversion efficiencies in the regime where $\Omega_2^{(eff,0)} \gg \Omega_1^{(eff,0)}$. This approach again leads to an increased the conversion efficiency compared to the case of *equal* effective Rabi frequencies. To generalize the analysis, we now treat different cases as an optimization problem (that maximize η), carried out with respect to T , α , and δ , for a set of different values of $\Omega_2^{(el,0)}$ within a range of $\Omega_2^{(el,0)} = 1.5 \times 10^7 - 10^{10} \text{ s}^{-1}$, and for a given value of $\Omega_1^{(el,0)} = 10^{10} \text{ s}^{-1}$. In terms of the effective Rabi frequencies, this corresponds to $\Omega_2^{(eff)}$ ranging from 1.5×10^6 to 10^9 s^{-1} , for a given $\Omega_1^{(eff,0)} = 2.1 \times 10^6 \text{ s}^{-1}$.

The results are summarized in Fig. 6 and in Table III where we give the corresponding optimum values of T , α , and δ , and the resulting maximum conversion efficiency η . For comparison, in the symmetric case of $\Omega_1^{(eff,0)} = \Omega_2^{(eff,0)} = 2.1 \times 10^6 \text{ s}^{-1}$ and $\delta = 0$, such that the optimization is carried out only with respect to T and α , the maximum conversion efficiency would be $\eta \simeq 0.14$ (at optimum $T = 0.46 \times 10^{-4} \text{ s}$ and $\alpha = 0.54$). This case is represented by the triangle, in Fig. 6.

Thus, we have shown that by introducing the possibility of varying the two-photon detuning δ and the Rabi frequency $\Omega_2^{(el,0)}$, the conversion efficiency can be increased almost by a factor of 4. This can be crucial for experimental observation of the phenomenon of coherent conversion of an atomic BEC into a molecular BEC, via STIRAP.

V. REALISTIC CONDENSATE MODELS

A. Uniform multi-level model

In our model for STIRAP we only treated the coupling of laser ω_1 to the free-bound transition $|1\rangle \leftrightarrow |3\rangle$ with Rabi frequency $\Omega_1 = \bar{\Omega}_1^{(el)} I_{1,3}$ together with the coupling of laser ω_2 to the bound-bound transition $|2\rangle \leftrightarrow |3\rangle$ with Rabi frequency $\Omega_2 = \bar{\Omega}_2^{(el)} I_{2,3}$. This approximation can only be valid if the laser ω_1 is far detuned from the $|2\rangle \leftrightarrow |3\rangle$ transition, and similarly – if the laser ω_2 is far detuned from the $|1\rangle \leftrightarrow |3\rangle$ transition. In addition, the two lasers have to be far detuned from transitions to any other vibrational levels $|v'\rangle$ (adjacent to $|3\rangle$) in the excited potential. We define the relevant detunings, for the simplest uniform case, as follows:

$$\begin{aligned} 2\Delta_{13,\omega_2} &= (E_3 - 2E_1)/\hbar - \omega_2, \\ \Delta_{23,\omega_1} &= (E_3 - E_2)/\hbar - \omega_1, \\ 2\Delta_{1v',\omega_1} &= (E_{v'} - 2E_1)/\hbar - \omega_1, \\ 2\Delta_{1v',\omega_2} &= (E_{v'} - 2E_1)/\hbar - \omega_2, \\ \Delta_{2v',\omega_1} &= (E_{v'} - E_2)/\hbar - \omega_1, \\ \Delta_{2v',\omega_2} &= (E_{v'} - E_2)/\hbar - \omega_2. \end{aligned} \quad (25)$$

In general, these cross-couplings – if included into the model – lead to incoherent radiative losses of atoms and molecules due to spontaneous emission. In order that these losses be negligible we require the respective detunings to be large enough. This requirement, however, may not be easily satisfied, as the magnitudes of the detunings are in principle limited from above by the characteristic distance between the adjacent vibrational levels of the excited molecular potential. In other words, increasing the detuning with respect to one transition will eventually bring the laser frequency to a resonance with respect to the nearby level. More importantly, these cross-couplings provide scattering pathways that are not cancelled out in a dark-state interference effect, so that their overall disruptive effect – over the adiabatically long pulse durations – may turn out to be rather large.

In order to estimate these effects, we therefore explicitly include all other relevant coupling processes into our model. In addition to losses, the incoherent couplings induce light shifts that effectively lead to a dephasing between the atomic and molecular condensates. Treating these, leads to the following additional terms in the

STIRAP equations, in same rotating frames as in Eqs. (9):

$$\frac{\partial\psi_1}{\partial t} = (\dots) - \frac{\alpha}{2}\psi_1 + i\beta_1\psi_1 - \frac{\Gamma_1}{2}|\psi_1|^2\psi_1 + i\bar{U}_{11}|\psi_1|^2\psi_1 - i\chi\psi_1^*\psi_2 + i\frac{\bar{\Omega}_2^{(el)}I_{1,3}}{\sqrt{2}}e^{-i2(\Delta_{13,\omega_2}-\Delta_1)t}\psi_1^*\psi_3, \quad (26)$$

$$\frac{\partial\psi_2}{\partial t} = (\dots) - \frac{\Gamma_2}{2}\psi_2 + i\beta_2\psi_1 - i\frac{\chi^*}{2}\psi_1^2 + i\frac{\bar{\Omega}_1^{(el)}I_{2,3}}{2}e^{-i(\Delta_{23,\omega_1}-\Delta_2)t}\psi_3, \quad (27)$$

$$\frac{\partial\psi_3}{\partial t} = (\dots) + i\frac{(\bar{\Omega}_2^{(el)}I_{1,3})^*}{2\sqrt{2}}e^{i2(\Delta_{13,\omega_2}-\Delta_1)t}\psi_1^2 + i\frac{(\bar{\Omega}_1^{(el)}I_{2,3})^*}{2}e^{i(\Delta_{23,\omega_1}-\Delta_2)t}\psi_2, \quad (28)$$

where (...) stand for the terms already present in the right hand sides of Eqs. (9). Here, the induced atom and molecule loss coefficients α , Γ_1 and Γ_2 , the light shift coefficients β_1 and β_2 , the nonlinear phase shift \bar{U}_{11} (which effectively leads to a modified atom-atom scattering length) and the effective parametric coupling χ are given by

$$\alpha = \frac{\gamma_A}{4} \left(\left| \frac{\Omega_1^{(A)}}{D_1} \right|^2 + \left| \frac{\Omega_2^{(A)}}{D_2} \right|^2 \right), \quad (29)$$

$$\Gamma_1 = \frac{\gamma}{4} \sum'_{v'} \left[\left| \frac{\bar{\Omega}_1^{(el)}I_{1,v'}}{2\Delta_{1v',\omega_1}} \right|^2 + \left| \frac{\bar{\Omega}_2^{(el)}I_{1,v'}}{2\Delta_{1v',\omega_2}} \right|^2 \right], \quad (30)$$

$$\Gamma_2 = \frac{\gamma}{4} \sum'_{v'} \left[\left| \frac{\bar{\Omega}_1^{(el)}I_{2v'}}{\Delta_{2v',\omega_1}} \right|^2 + \left| \frac{\bar{\Omega}_2^{(el)}I_{2v'}}{\Delta_{2v',\omega_2}} \right|^2 \right], \quad (31)$$

$$\beta_1 = \frac{|\Omega_1^{(A)}|^2}{4D_1} + \frac{|\Omega_2^{(A)}|^2}{4D_2}, \quad (32)$$

$$\beta_2 = \sum'_{v'} \left[\frac{|\bar{\Omega}_1^{(el)}I_{2,v'}|^2}{4\Delta_{2v',\omega_1}} + \frac{|\bar{\Omega}_2^{(el)}I_{2,v'}|^2}{4\Delta_{2v',\omega_2}} \right], \quad (33)$$

$$\bar{U}_{11} = \sum'_{v'} \left[\frac{|\bar{\Omega}_1^{(el)}I_{1,v'}|^2}{8\Delta_{1v',\omega_1}} + \frac{|\bar{\Omega}_2^{(el)}I_{1,v'}|^2}{8\Delta_{1v',\omega_2}} \right], \quad (34)$$

$$\chi = -\frac{\bar{\Omega}_1^{(el)}\bar{\Omega}_2^{(el)*}}{2\sqrt{2}} \sum'_{v'} \frac{I_{1,v'}I_{2,v'}^*}{2\Delta_{1v',\omega_1}}. \quad (35)$$

where $D_1 = \omega_0 - \omega_1$ and $D_2 = \omega_0 - \omega_2$ represent the detunings of lasers ω_1 and ω_2 from the resonance frequency ω_0 of the atomic transition between the dissociation limits of the ground and excited potentials. In addition, $\gamma_A = \gamma/2$ is the atomic spontaneous decay rate, and $\Omega_1^{(A)}$ and $\Omega_2^{(A)}$ are the atomic Rabi frequencies which we take $\Omega_i^{(A)} = \bar{\Omega}_i^{(el)}/\sqrt{2}$.

The coefficients α , Γ_i , β_i , \bar{U}_{11} and χ are obtained by explicitly treating all other levels in the excited potential, adjacent to $|3\rangle$, followed by the procedure of adiabatic elimination. The coefficients also include the contributions from Raman type of couplings $|1\rangle \leftrightarrow |v'\rangle$ by the ω_1 -laser and $|2\rangle \leftrightarrow |v'\rangle$ by ω_2 -laser. In principle, these additional Raman couplings could be treated exactly like the primary STIRAP transition via $|3\rangle$, i.e. taking place via the dark-state interference effect, except that the transitions have much larger one-photon detuning. This would require an adiabaticity condition of the form of Eq. (17) that includes the one-photon detuning, implying that a larger value of the product $\Omega_i^{(eff,0)}T$ is needed. However, $\Omega_i^{(eff,0)}T$ can not be made arbitrarily large, as we discussed earlier. Therefore our approach is to treat these extra Raman couplings as loss and dephasing processes, rather than to include them into the adiabatic passage scheme. The contribution of these couplings to the effective atom-molecule conversion rate, described by χ , is negligibly small compared to the conversion rate due to the parimary Raman transition via $|3\rangle$.

The relevant transitions that stand behind these coefficients are illustrated in Fig. 7. For example, the coefficient α describes the process of atomic absorption from either of the two Raman lasers, that incoherently produce excited atoms followed by spontaneous emission loss. The coefficient Γ_1 is due to ordinary photoassociation when pairs of atoms from the condensate are transferred (again by either of the two Raman lasers) into an excited molecular state which can then spontaneously dissociate into a pair of hot (non-condensed) atoms. The effective rate of this non-linear loss is $\Gamma_1 n_1$. Finally, the coefficient Γ_2 describes incoherent production of excited molecules which can then spontaneously decay into ground state molecules in ro-vibrational states other than the one targeted by the stimulated Raman transitions.

The summations in the expressions for Γ_i , β_2 , \bar{U}_{11} and χ are carried out over all the excited levels v' except the resonant level $|3\rangle$ which itself participates in STIRAP, rather than being adiabatically eliminated. The effects of losses and light shifts due to the cross-couplings to the level $|3\rangle$ itself are implicitly described by the last terms in the rhs of Eqs. (26)-(28). Subsequently, we will estimate the combined effects of all levels in which case the contribution of the level $|3\rangle$ is estimated by similar terms to the ones included in Γ_i , β_2 , \bar{U}_{11} , except that the detunings $\Delta_{v'1,\omega_2}$ and $\Delta_{v'2,\omega_1}$ are replaced by Δ_{13,ω_2} and Δ_{23,ω_1} , respectively, and $I_{i,v'}$ are replaced by $I_{i,3}$.

Separating out the time dependences of the two Rabi

frequencies, the above coefficients can be rewritten as:

$$\alpha = \alpha^{(1)} e^{-2(t-t_1)^2/T^2} + \alpha^{(2)} e^{-2(t-t_2)^2/T^2}, \quad (36)$$

$$\Gamma_i = \Gamma_i^{(1)} e^{-2(t-t_1)^2/T^2} + \Gamma_i^{(2)} e^{-2(t-t_2)^2/T^2}, \quad (37)$$

$$\beta_i = \beta_i^{(1)} e^{-2(t-t_1)^2/T^2} + \beta_i^{(2)} e^{-2(t-t_2)^2/T^2}, \quad (38)$$

$$\bar{U}_{11} = \bar{U}_{11}^{(1)} e^{-2(t-t_1)^2/T^2} + \bar{U}_{11}^{(2)} e^{-2(t-t_2)^2/T^2}, \quad (39)$$

$$\chi = \chi_0 e^{-(t-t_1)^2/T^2} e^{-(t-t_2)^2/T^2}, \quad (40)$$

where the peak values are, respectively:

$$\alpha^{(i)} = \frac{\gamma}{4} \left| \frac{\Omega_i^{(A,0)}}{D_i} \right|^2, \quad (41)$$

$$\Gamma_1^{(i)} = \frac{\gamma}{4} \sum'_{v'} \left| \frac{\bar{\Omega}_i^{(el,0)} I_{1,v'}}{2\Delta_{1v',\omega_i}} \right|^2, \quad (42)$$

$$\Gamma_2^{(i)} = \frac{\gamma}{4} \sum'_{v'} \left| \frac{\bar{\Omega}_i^{(el,0)} I_{2,v'}}{\Delta_{2v',\omega_i}} \right|^2, \quad (43)$$

$$\beta_1^{(i)} = \frac{|\Omega_i^{(A,0)}|^2}{4D_i}, \quad (44)$$

$$\beta_2^{(i)} = \sum'_{v'} \frac{|\bar{\Omega}_i^{(el,0)} I_{2,v'}|^2}{4\Delta_{2v',\omega_i}}, \quad (45)$$

$$\bar{U}_{11}^{(i)} = \sum'_{v'} \frac{|\bar{\Omega}_i^{(el,0)} I_{1,v'}|^2}{4\Delta_{1v',\omega_i}}. \quad (46)$$

$$\chi_0 = -\frac{\bar{\Omega}_1^{(el,0)} \bar{\Omega}_2^{(el,0)*}}{2\sqrt{2}} \sum'_{v'} \frac{I_{1,v'} I_{2,v'}^*}{2\Delta_{1v',\omega_1}}. \quad (47)$$

The reason for this separation is that the two terms in each coefficient act during different time intervals, corresponding to the first and the second pulse in STIRAP. Accordingly, one has to distinguish their disruptive effect during the duration of the corresponding pulses. For example the molecule loss term $\Gamma_2^{(2)}$ acts during the first Raman pulse (of frequency ω_2) when the molecular field is not populated yet. As a result, the coefficient $\Gamma_2^{(2)}$ is

not so disruptive. On the other hand, the molecule loss term $\Gamma_2^{(1)}$ is much more important since it acts during the second Raman pulse (with frequency ω_1) when the population of the molecular condensate becomes high. If the value of $\Gamma_2^{(1)}$ is too large, one can easily lose all this population during the ω_1 -pulse.

In order that the radiative losses and dephasing due to light shifts be negligible over the duration of STIRAP, the time scales associated with the coefficients α , $\Gamma_1 n_1$, Γ_2 , and the induced *relative* phases must be much larger than the duration of pulses in STIRAP, i.e.

$$\left[\alpha^{(i)} \right]^{-1} \gg T, \quad (48)$$

$$\left[\Gamma_1^{(1)} n_1 \right]^{-1} \gg T, \quad (49)$$

$$\left[\left(\Gamma_1^{(2)} + \frac{\gamma}{4} \left| \frac{\bar{\Omega}_2^{(el,0)} I_{1,3}}{2\Delta_{13,\omega_2}} \right|^2 \right) n_1 \right]^{-1} \gg T, \quad (50)$$

$$\left[\Gamma_2^{(1)} + \frac{\gamma}{4} \left| \frac{\bar{\Omega}_1^{(el,0)} I_{2,3}}{\Delta_{23,\omega_1}} \right|^2 \right]^{-1} \gg T, \quad (51)$$

$$\left[\Gamma_2^{(2)} \right]^{-1} \gg T, \quad (52)$$

$$\left| \left(\beta_2^{(1)} + \frac{|\bar{\Omega}_1^{(el,0)} I_{2,3}|^2}{4\Delta_{23,\omega_1}} \right) - 2\beta_1^{(1)} \right|^{-1} \gg T, \quad (53)$$

$$\left| \beta_2^{(2)} - 2\beta_1^{(2)} \right|^{-1} \gg T. \quad (54)$$

This will guarantee that the pulses are switched off before the losses and dephasings can have their disruptive effect. The influence of the nonlinear phase shift due to $\bar{U}_{11}^{(i)}$ can be ignored simply on the grounds of $\bar{U}_{11}^{(i)} \ll U_{11}$ which is the case we encounter in our analysis.

In the above conditions involving the coefficients $\Gamma_1^{(2)}$, $\Gamma_2^{(1)}$, and $\beta_2^{(1)}$, we have included additional terms which are the contributions from the incoherent cross-couplings $1 \leftrightarrow 3$ by the laser ω_2 and $2 \leftrightarrow 3$ by the laser ω_1 . As we mentioned earlier, these processes are treated explicitly by the last terms in the rhs of Eqs. (26)-(28). However, their overall effect can be described by expressions similar to the corresponding terms in the coefficients $\Gamma_1^{(2)}$, $\Gamma_2^{(1)}$, and $\beta_2^{(1)}$. Therefore these additional contributions must be included in the above conditions, as they play an important role for correct estimates of the overall degree of disruption due to incoherent couplings.

Our goal now is in performing a realistic analysis of the above coefficients for the $^{87}\text{Rb}_2$ molecule under consideration, and in finding appropriate target levels for the Raman transitions in STIRAP so that the disruptive effects are minimized. This is done using the results of calculation [17] of the dipole matrix elements, energy eigenvalues, and the Franck-Condon overlap integrals for model potentials that closely approximate the $^{87}\text{Rb}_2$ ground $^3\Sigma^+$ potential and the O_g^- symmetry excited potential. The calculation treats 205 ro-vibrational levels in the excited potential (which we label by $v' = 0, 1, 2, \dots, 204$) and 39 levels ($v = 0, 1, 2, \dots, 38$) in the ground potential.

Within such a large range of target levels that the Raman transitions can be tuned to, several possibilities can be readily eliminated to simplify the search. For example, Raman transitions via one of the highly excited levels ($v' \gtrsim 190$) will suffer from large values of the atomic loss coefficient α since the detunings D_i will be small, and as a result the condition $[\alpha^{(i)}]^{-1} \gg T$ will not be satisfied. On the other hand, transitions via low excited states ($v' \lesssim 160$) will have very small values of the free-bound Franck-Condon overlap integral, $I_{1,v'} \lesssim 0.5 \times 10^{-14} \text{ m}^{3/2}$. This in turn will result in small effective Rabi frequency $\Omega_1^{(eff,0)}$ (using reasonable values of the intensity of the laser ω_1 and the density n_1), so that the adiabaticity condition $\Omega_1^{(eff,0)} T \gg 1$ is not satisfied.

In general, the behavior of the coefficients $\Gamma_1^{(i)}$, $\Gamma_2^{(i)}$, and $\beta_2^{(i)}$ is not of a trivial character. Each particular choice of the final state $|v\rangle$ in the ground potential which we designate as $|2\rangle$ will result in different sets of the detunings of the Raman lasers with respect to couplings to different excited levels. Further complications emerge from the oscillatory behavior of the Franck-Condon overlap integrals, as shown in Fig. 8. This means that the contribution of the levels nearest to $|3\rangle$, having the smallest detunings, may not necessarily give the leading term in the sums over v' , since the further detuned levels may have larger Franck-Condon overlaps thus resulting in comparable contributions to the coefficients. In addition, different terms in the expression for $\beta_2^{(i)}$ will depend on the sign of the respective detuning, so that they may add up into either a positive or negative value of $\beta_2^{(i)}$.

Thus our analysis consists of a calculation of all the above coefficients for different levels $|v\rangle$ and $|v'\rangle$, and subsequent identification of an optimum target level that satisfies the conditions (48)-(54) as closely as possible. For each level $|v\rangle \equiv |2\rangle$ in the ground potential we scan the Raman transitions through different levels $|v'\rangle$ in the excited potential, treating this as $|3\rangle$ and carrying out the summations over the remaining levels.

The calculation is done for $\Omega_1^{(el,0)} = 10^{10} \text{ s}^{-1}$ and $\Omega_2^{(el,0)} = 10^9 \text{ s}^{-1}$. To simplify the analysis we consider the case of $\Delta_1 = 0$ and $\delta = 0$, i.e. we only treat cases when the primary Raman transition is resonant. Once the optimum level is identified, we can subsequently fine tune the two-photon detuning δ for optimum conversion.

$\alpha^{(1)}$	51.43 s^{-1}
$\alpha^{(2)}$	0.5398 s^{-1}
$\Gamma_1^{(1)}$	$3.010 \times 10^{-24} \text{ m}^3/\text{s}$
$\Gamma_1^{(2)}$	$3.014 \times 10^{-26} \text{ m}^3/\text{s}$
$\Gamma_2^{(1)}$	466.7 s^{-1}
$\Gamma_2^{(2)}$	4.645 s^{-1}
$\beta_1^{(1)}$	$2.948 \times 10^6 \text{ s}^{-1}$
$\beta_1^{(2)}$	$3.020 \times 10^4 \text{ s}^{-1}$
$\beta_2^{(1)}$	$5.652 \times 10^6 \text{ s}^{-1}$
$\beta_2^{(2)}$	$5.969 \times 10^4 \text{ s}^{-1}$
$(\gamma/4) \left \bar{\Omega}_2^{(el,0)} I_{1,3} \right ^2 / 2\Delta_{13,\omega_2} ^2$	$7.96 \times 10^{-25} \text{ m}^3/\text{s}$
$(\gamma/4) \left \bar{\Omega}_1^{(el,0)} I_{2,3} \right ^2 / \Delta_{23,\omega_1} ^2$	375.9 s^{-1}
$ \bar{\Omega}_1^{(el,0)} I_{2,3} ^2 / (4\Delta_{23,\omega_1})$	$2.57 \times 10^5 \text{ s}^{-1}$
χ_0	$-9.25 \times 10^{-9} \text{ m}^{3/2}/\text{s}$

TABLE IV. Calculated values of the loss and light shift coefficients for Raman transitions tuned to the ground $v = 35$ and excited $v' = 177$ levels.

Provided that the order of magnitude of the optimum δ is $|\delta| \sim 10^4 \text{ s}^{-1}$ as found in the examples of sub-sections IV. B and C, this subsequent fine tuning will have no effect on the results of calculation of the loss and light shift coefficients, since these involve detunings Δ_{iv',ω_j} that typically have much larger magnitudes, $|\Delta_{iv',\omega_j}| \gg |\delta|$.

The most favorable case that we find corresponds to tuning the Raman transitions to $v' = 177$ in the excited potential bound by -22.23 cm^{-1} or $-4.1903 \times 10^{12} \text{ s}^{-1}$ from the dissociation limit, and $v = 35$ in the ground potential bound by -8.05 GHz or $-5.058 \times 10^{10} \text{ s}^{-1}$. The binding energy of the level $v = 35$ sets up the frequency difference $\omega_2 - \omega_1 = 5.058 \times 10^{10} \text{ s}^{-1}$, and the values of all relevant detunings. The nearby levels around $v' = 177$ in the excited potential are separated by about $4.2 \times 10^{11} \text{ s}^{-1}$, which is much larger than $\omega_2 - \omega_1$. For this arrangement of the target levels, the resonant Franck-Condon overlap integrals are equal to $I_{1,3} = 1.05 \times 10^{-14} \text{ m}^{3/2}$ and $I_{2,3} = 0.0228$, so that the effective peak Rabi frequencies are equal to: $\Omega_1^{(eff,0)} = 2.18 \times 10^6 \text{ s}^{-1}$, for $n_1(0) = 4.3 \times 10^{20} \text{ m}^{-3}$, and $\Omega_2^{(eff,0)} = 2.28 \times 10^7 \text{ s}^{-1}$. The resulting values of calculated loss and light shift coefficients are given in Table IV.

An important factor in minimizing the most significant loss coefficient $\Gamma_2^{(1)}$ and its “cousin” term in Eq. (51) is the relatively small value of $I_{2,3}$ and of the Franck-Condon overlaps $I_{2,v'}$ of the closest nearby levels. While this is favorable for the undesired loss terms, the small value of $I_{2,3}$ also affects the strength of the bound-bound coupling of the primary Raman transition, $\Omega_2^{(eff,0)} = \Omega_2^{(el,0)} I_{2,3}$, which must be kept large. However, the small $I_{2,3}$ -value is compensated here by a strong bare electronic Rabi frequency $\Omega_2^{(el,0)} = 10^9 \text{ s}^{-1}$ so that $\Omega_2^{(eff,0)}$ is still large and the adiabaticity condition is maintained.

Using the above parameter values and simulating the STIRAP equations with the additional terms given by Eqs. (26)-(28), results in about 42% conversion efficiency ($\eta = 0.42$), which is rather high and is an encouraging result. In this simulation, the estimated optimum pulse duration T , the pulse delay coefficient α , and the two-photon detuning δ , were taken as follows: $T = 1.7 \times 10^{-4}$ s $^{-1}$, $\alpha = 1.53$, and $\delta = 4 \times 10^4$ s $^{-1}$. The effective Rabi frequencies and the particle number densities for this calculation are given in Figs. 9 (a) and (b).

B. Non-uniform condensates

The final step in our analysis is to include the trap potential and the kinetic energy terms and simulate the full set of coupled equations (6) in three space dimensions. We consider spherically symmetric trap potentials $V_i(\mathbf{x}) = E_i + (m_i/2)\omega_i^2|\mathbf{x}|^2$ and choose the trap oscillation frequencies ω_i equal to each other: $\omega_i/2\pi = 100$ Hz ($i = 1, 2, 3$). Including these terms, we simulate Eqs. (6) assuming an initial condition of a pure atomic BEC with a peak density of $n_1(\mathbf{x}=0, 0) = 4.3 \times 10^{20}$ m $^{-3}$ at the trap center. This corresponds to the total initial number of atoms $N_1 = \int d^3\mathbf{x}|\psi(\mathbf{x}, 0)|^2$ equal to $N_1 = 10^6$.

We note that the characteristic time scale associated with the trap potential can be estimated as $t_\omega = 1/\omega \simeq 1.6 \times 10^{-3}$ s. The time scale associated with the kinetic energy term is estimated from the ‘healing’ length $l_h \sim \sqrt{\hbar t_h/m_1}$ which corresponds to a healing time scale of t_h . Under adiabatic conversion of an equilibrium (Thomas-Fermi like) atomic BEC, this healing time scale coincides with the dephasing time t_{ph} associated with the mean field energy potential and discussed before. Both these time scales (t_ω and t_h) are longer than the duration of pulses in STIRAP we employed earlier. Therefore, addition of these terms can not dramatically change the results and conclusions obtained above for uniform condensates.

To show this we first consider the idealized three-level model with parameter values given in Tables I and II, i.e. the case of equal and relatively strong effective Rabi frequencies. The results of simulations of Eqs. (6) are shown in Figs. 10 and 11, where we see a rather high conversion efficiency $\eta \simeq 0.91$. This should be compared with the uniform condensates result of Fig. 3.

Next, we consider the case of more realistic parameter values (lower Rabi frequencies), and include the effects of incoherent radiative losses and dephasings as described in the previous sub-section. Using the calculated values of all relevant parameters for the Raman transitions tuned to $v' = 177$ and $v = 35$, and adding the trap potential and kinetic energy terms to the earlier Eqs. (26)-(28), we obtain a conversion efficiency of $\eta \simeq 0.32$ as shown in Fig. 12. This is 10% lower than the efficiency in the corresponding homogeneous case of Fig. 9, but still is a rather encouraging result given the fact that 32%

conversion of about 5×10^5 atoms would give a molecular BEC with the total of 8×10^4 molecules, with a peak density of about 10^{20} m $^{-3}$.

VI. SUMMARY

To summarize, STIRAP is a potential route towards the coherent conversion of an atomic to a molecular BEC. This process involves stimulated emission of molecules, and is very different to normal chemical kinetics. As such, it is a form of ‘superchemistry’ [1]. STIRAP in an atomic BEC can be treated in a very similar way to normal STIRAP, by introducing an effective Rabi frequency for the first photo-association transition. A potential difficulty is the relatively low values of the effective Rabi frequency in the first or photo-association transition. This can be regarded as physically due to the low densities of atoms in a typical weakly interacting BEC, compared with atoms in a molecule. This means that the corresponding Franck-Condon coefficient, after multiplying by the relevant BEC amplitude, has a very small value. Thus, the laser intensities required may be quite high, in order to obtain Rabi frequencies comparable to those used in atomic transitions.

This by itself is not critical, since deep in the adiabatic limit it is normally permissible to use low Rabi frequencies, as long as the associated time-scales are long enough. From this point of view, the use of STIRAP, and consequent reduction of spontaneous emission, is a physically sensible idea. However, including S-wave scattering or mean-field processes into the model for STIRAP sets up a characteristic two-photon dephasing time scale, so that the pulse durations in STIRAP have to be *shorter* than a certain critical value. Short pulse durations necessarily involve high values for the effective Rabi frequencies in the usual symmetric case of $\Omega_1^{(eff,0)} = \Omega_2^{(eff,0)}$, thus requiring a very high laser power for the first transition - if the adiabaticity condition is to be maintained.

In order to ease this demanding requirement and be able to achieve highest possible conversion efficiency at smaller total laser power, we propose to use an off-resonance operation (thus cancelling part of the mean-field detuning effect) and effective Rabi frequencies $\Omega_1^{(eff,0)}$ and $\Omega_2^{(eff,0)}$ of different magnitudes. This has the effect of dramatically increasing coherent molecule production, in a physically accessible regime of moderate laser intensity. Further improvements may be possible by tailoring the input pulse frequencies to the time-dependent two-photon detuning, caused by inter-atomic and intermolecular scattering.

Finally, we stress the importance of radiative losses and dephasing due to incoherent processes that occur during STIRAP. These processes are usually assumed to be negligible in ordinary STIRAP between purely atomic or molecular states. In the present case of coupled atomic/molecular BECs, this assumption can not be eas-

ily justified since the free-bound transition typically involves a relatively low effective Rabi frequency, which necessitates long pulse durations. Instead, we find that the incoherent couplings can be rather destructive unless special care is taken to minimize their effect. This involves detailed knowledge of the structure of the free-bound and bound-bound transitions and subsequent identification of optimum target levels in STIRAP, so that the overall conversion efficiency remains comparable to the predictions of the simplified three-level model.

ACKNOWLEDGMENTS

The authors gratefully acknowledge the ARC for the support of this work.

[1] D. Heinzen, R. Wynar, P. D. Drummond, and K. V. Kheruntsyan, Phys. Rev. Lett. **84**, 5029 (2000).

[2] K. V. Kheruntsyan and P. D. Drummond, Phys. Rev. A **58**, R2676 (1998).

[3] P. D. Drummond, K. V. Kheruntsyan, and H. He, Phys. Rev. Lett. **81**, 3055 (1998).

[4] J. Javanainen and M. Mackie, Phys. Rev. A **59**, R3186 (1999).

[5] R. H. Wynar, R. S. Freeland, D. J. Han, C. Ryu, and D. J. Heinzen, Science **287**, 1016 (2000).

[6] Y. B. Band and P. Julienne, Phys. Rev. A **51**, R4317 (1995); A. Vardi, D. Abrashkevich, E. Frishman, and M. Shapiro, Chem. Phys. **107**, 6166 (1997); J. M. Vogels *et al.*, Phys. Rev. A **51**, R1067 (1997); P. S. Julienne, K. Burnett, Y. B. Band, and W. C. Stwalley, Phys. Rev. A **58**, R797 (1998); R. Côté and A. Dalgarno, Chem. Phys. Lett. **279**, 50 (1997).

[7] P. Tommasini, E. Timmermans, M. Hussein, and A. Kerman, cond-mat/9804015; E. Timmermans *et al.*, Phys. Rev. Lett. **83**, 2691 (1999); V. A. Yurovsky, A. Ben-Reuven, P. S. Julienne, and C. J. Williams, Phys. Rev. A **60**, R765 (1999); F. A. van Abeelen and B. J. Verhaar, Phys. Rev. Lett. **83**, 1550 (1999); F. H. Mies, E. Tiesinga, and P. S. Julienne, Phys. Rev. A **61**, 022721 (2000).

[8] E. Tiesinga, B. J. Verhaar, and H. T. C. Stoof, Phys. Rev. A **47**, 4114 (1993); E. Tiesinga, A. J. Moerdijk, B. J. Verhaar, and H. T. C. Stoof, Phys. Rev. A **46**, R1167 (1992); A. J. Moerdijk, B. J. Verhaar, and A. Axelsson, Phys. Rev. A **51**, 4852 (1995); J. M. Vogels *et al.*, Phys. Rev. A **56**, R1067 (1997);

[9] S. Inouye *et al.*, Nature **392**, 151 (1998); Ph. Courteille, R. S. Freeland, and D. Heinzen, Phys. Rev. Lett. **81**, 69 (1998); J. L. Roberts *et al.*, Phys. Rev. Lett. **81**, 5109 (1998); J. Stenger, Phys. Rev. Lett. **82**, 2422 (1999).

[10] M. Mackie, R. Kowalski, and J. Javanainen, Phys. Rev. Lett. **84**, 3803 (2000).

[11] P. O. Fedichev *et al.*, Phys. Rev. Lett. **77**, 2913 (1996); K. Burnett, P. S. Julienne, and K.-A. Suominen, Phys. Rev. Lett. **77**, 1416 (1996); J. L. Bohn and P. S. Julienne, Phys. Rev. A **56**, 1486 (1997).

[12] A. L. Fetter and J. D. Walecka, *Quantum theory of many-particle systems* (McGraw-Hill, New York, 1991); A. A. Abrikosov, L. P. Gorkov, and I. E. Dzyaloshinski, *Methods of Quantum Field Theory in Statistical Physics* (Dover, New York, 1963); N. P. Proukakis, K. Burnett, and H. T. C. Stoof, Phys. Rev. A **57**, 1230 (1998).

[13] M. Holland, J. Park, and R. Walser, cond-mat/0005062.

[14] J. J. Hope, M. K. Olsen, and L. I. Plimak, Phys. Rev. A **63**, 043603 (2001).

[15] K. Bergman, H. Theuer, and B. W. Shore, Rev. Mod. Phys. **70**, 1003 (1998); K. Bergmann and B. W. Shore, in *Molecular Dynamics and Spectroscopy by Stimulated Emission Pumping*, H-L Dai and R. W. Field, Eds. (World Scientific, 1995).

[16] J. M. Vogels *et al.*, Phys. Rev. A **56**, R1067 (1997).

[17] R. H. Wynar, PhD Thesis, University of Texas at Austin, 2000; S. J. J. M. F. Kokkelmans and B. J. Verhaar, private communication.

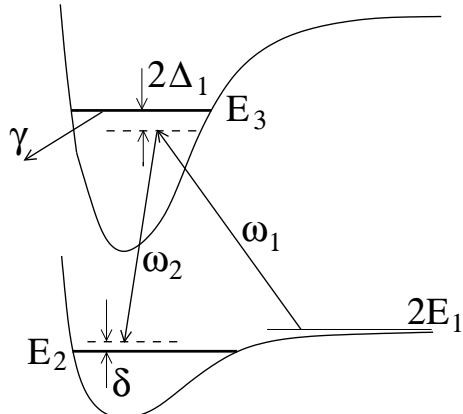


FIG. 1. Diagrammatic representation of the free-bound and bound-bound transitions in STIRAP.

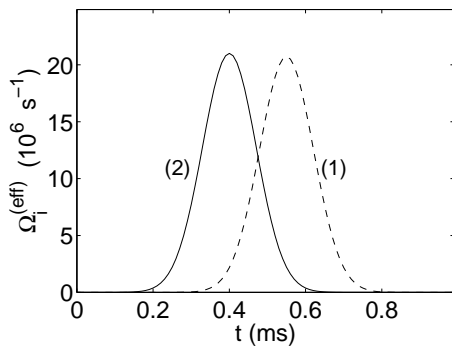


FIG. 2. The Rabi frequencies $\Omega_i^{(eff)}(t)$ for the Raman transitions, with the peak values of $\Omega_1^{(eff,0)} = \Omega_2^{(eff,0)} = 2.1 \times 10^7 \text{ s}^{-1}$, pulse durations $T = 10^{-4} \text{ s}$, and a delay coefficient of $\alpha = 1.5$.

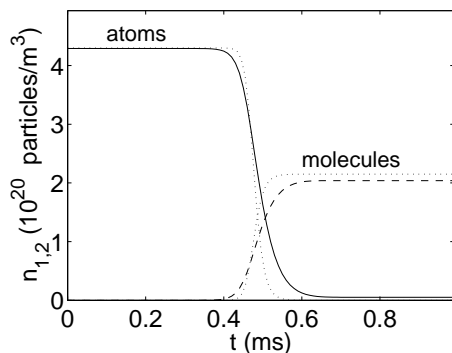


FIG. 3. Efficient conversion of an atomic condensate into a molecular condensate during STIRAP as obtained by simulating Eqs. (21), with an initial atom number density $n_1(0) = 4.3 \times 10^{20} \text{ m}^{-3}$. Other parameter values are as in Fig. 2, and Tables I and II. The solid line indicates atomic density, the dashed line the molecular density, and the dotted line the analytic result in the adiabatic limit.

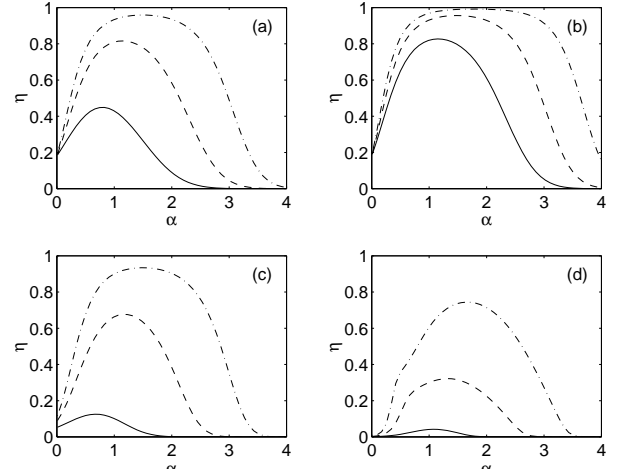


FIG. 4. The conversion efficiency η as a function of relative delay α , for: (a) $T = 10^{-4} \text{ s}$ and $U_{ij} = 0$; (b) $T = 10^{-3} \text{ s}$ and $U_{ij} = 0$; (c) $T = 10^{-4} \text{ s}$ and U_{ij} as in Table II; (d) $T = 10^{-3} \text{ s}$ and U_{ij} as in Table II. The full, dashed, and dashed-dotted lines correspond to effective Rabi frequencies $\Omega_1^{(eff,0)} = \Omega_2^{(eff,0)}$ equal to $2.1 \times 10^6 \text{ s}^{-1}$, $6.3 \times 10^6 \text{ s}^{-1}$, and $2.1 \times 10^7 \text{ s}^{-1}$. Other parameter values are as in Table I.

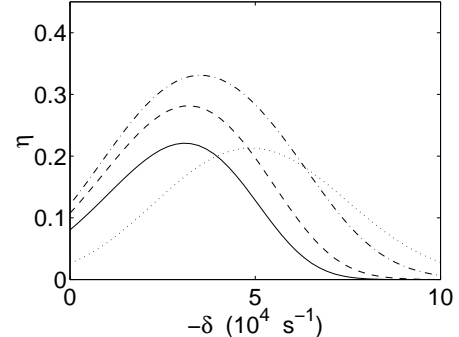


FIG. 5. The conversion efficiency η as a function of $-\delta$, for $\Omega_1^{(eff,0)} = \Omega_2^{(eff,0)} = 2.1 \times 10^6 \text{ s}^{-1}$, $T = 10^{-4} \text{ s}$ and different delay coefficients: $\alpha = 0.2$ (full line), $\alpha = 0.4$ (dashed line), $\alpha = 0.8$ (dashed-dotted line), $\alpha = 1.5$ (dots). Other parameter values are as in Tables I and II.

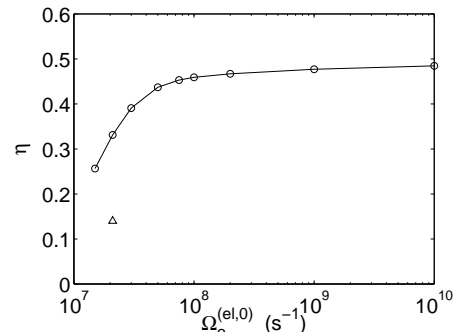


FIG. 6. The maximum conversion efficiency η versus $\Omega_2^{(el,0)}$ (the evaluated points are represented by circles), for $\Omega_1^{(el,0)} = 10^{10} \text{ s}^{-1}$ and the corresponding optimum values of T , α , and δ as given in Table III. The triangle gives the result of an optimization with $\delta = 0$.

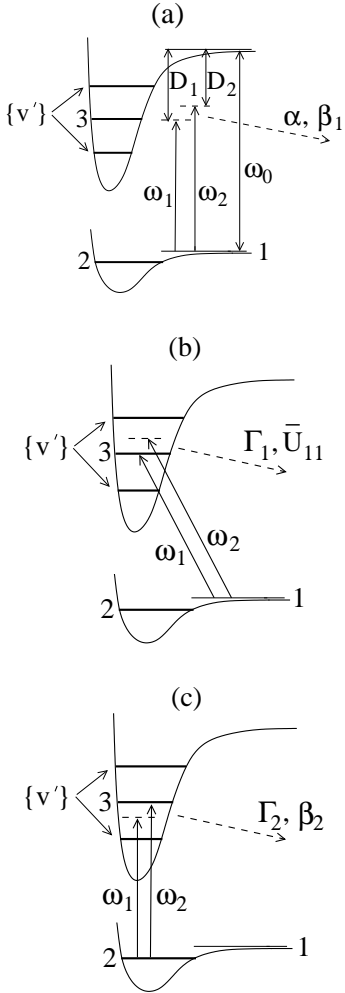


FIG. 7. Diagrammatic representation of incoherent scattering processes resulting in induced losses and light shifts.

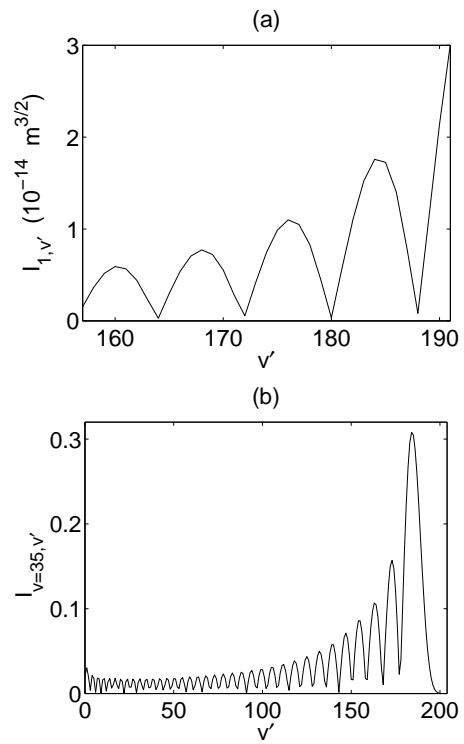


FIG. 8. Free-bound (a) and bound-bound (b) Franck-Condon overlap integrals, $I_{1,v'}$ and $I_{v=35,v'}$, as a function of the vibrational quantum number v' .

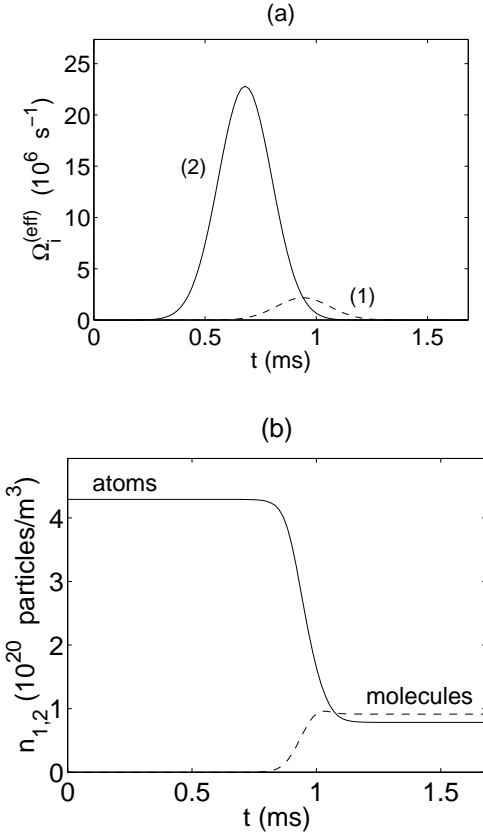


FIG. 9. (a) Optimum effective Rabi frequencies for STI-RAP in the multi-level model. (b) Resulting densities in the uniform condensates case.

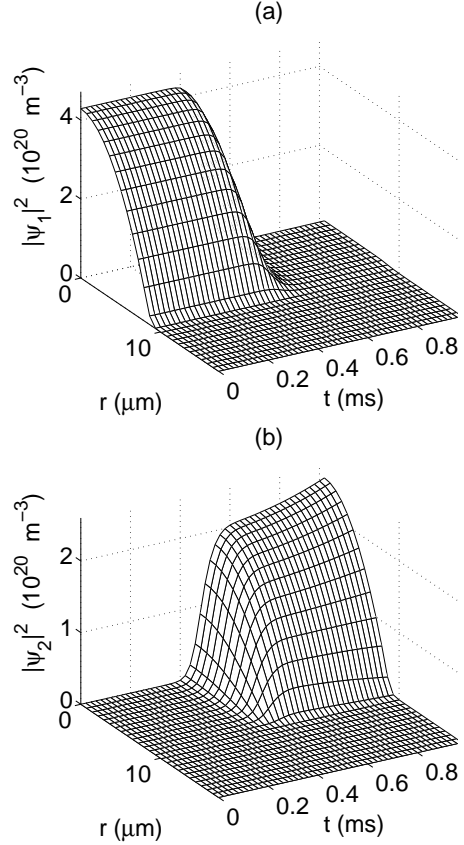


FIG. 10. Densities $n_i(\mathbf{x}, t) = |\psi_i(\mathbf{x}, t)|^2$ of the atomic (a) and molecular (b) condensates in a trap as a function of time t and the radial distance $r = |\mathbf{x}|$ from the trap center. The applied pulses are as in Fig. 2, and other parameter values are given in Tables I and II. The result is for the idealized three-level model.

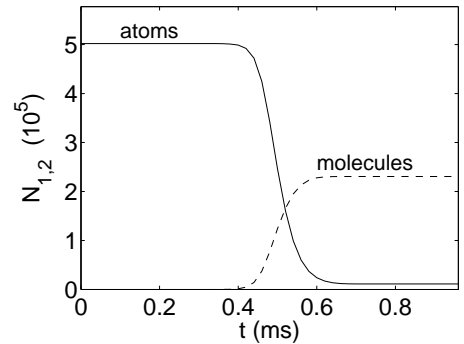


FIG. 11. Integrated occupation numbers $N_i(t) = \int d\mathbf{x} |\psi_i(\mathbf{x}, t)|^2$ of the atomic (solid line) and the molecular (dashed line) fields as a function of time t , for the parameter values of Fig. 10.

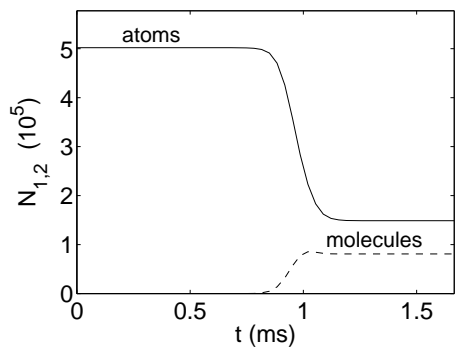


FIG. 12. Same as in Fig. 11 but for the parameter values of the complete multi-level model and a three-dimentional trap geometry. The resulting conversion efficiency can be compared with the uniform condensates case of Fig. 9 (b).